NATIONAL AERONAUTICS AND SPACE ADMINISTRATION

Technical Report No. 32-877

Digital Video-Data Handling

Robert Nathan

Karl W Linnes

K. W. Linnes, *Manager*
Space Instrument Systems Section

JET PROPULSION LABORATORY
CALIFORNIA INSTITUTE OF TECHNOLOGY
PASADENA, CALIFORNIA

January 5, 1966

FIGURES (Cont'd)

6. Simple notch filter 8
7. Mathematically correct version of simple notch filter 8
8. (a) Noisy picture, (b) Two-dimensional frequency transform of picture 9
9. Scan-line filter 9
10. System frequency-response curve 10
11. *Ranger VIII* frame after normal clean-up, (b) *Ranger VIII* frame with sine-wave frequency correction 10
12. Correction frequency-response curve 11
13. (a) *Ranger VII* P_1 frame before (left) and after clean-up, (b) *Mariner* frame 1 before (left) and after clean-up 13

ABSTRACT

A technique has been developed which makes it possible to perform accurate, detailed operations and analyses upon digitized pictorial data. Television pictures transmitted from the *Ranger* and *Mariner* spacecraft have been significantly improved in clarity by correcting those system distortions which affect photometric, geometric, and frequency fidelity. Various classes of structured noise have also been detected and removed digitally by means of newly devised two-dimensional filters. Although mathematically the filters are easier to describe in the frequency domain, they are more effectively applied as a convolution operation on the original digitized photographs. The cleaned-up, enhanced pictures are then used by the computer for further interpretive and statistical analyses.

I. OBJECTIVES

It is the function of the video-data-handling system to reproduce the original scene of transmitted television pictures as faithfully as possible in terms of resolution, geometry, photometry, and perhaps color. The difficulty lies in overcoming limitations imposed by the noise, distortions, and information bandwidth of the system. These corrections are performed by computer after the pictures have been digitized. The pictures in cleaned-up form can be enhanced in contrast and used for detailed visual photo-interpretation.

Once the pictures have been corrected, information can be extracted from them. Since the pictures are now in digital form, some of the analyses can be performed by the computer. In the case of the Moon (where surface photometric properties can be considered reasonably homogeneous), the slope and relative elevation can be calculated from the relation of the surface to the brightness as a function of Sun, observation point, and surface location.

II. PROBLEMS

There are several significant differences between taking a picture with a film camera and a television vidicon camera. Assuming that the lenses are not the limiting factor, the differences appear in the manner in which the image projected onto the receiving surface is sensed. Spectral and dynamic sensitivity and linearity differ. Grain size limits film resolution, and scanning-beam spot size limits vidicon resolution. Geometric fidelity is worse in the vidicon scanning camera than in film. Noise in transmission is unique to electrically encoded pictures.

There are several other problems unique to film, but emphasis here is upon those weaknesses of television systems which add to the photo-interpretive and map-making difficulties.

Several years ago, when the *Ranger* effort was first proposed, no known methods existed of performing by analog means alone all the desired operations of clean-up, calibration correction, and information extraction on video data. The most practicable approach to the solution of these problems available at that time was to digitize the data and perform these operations on a computer. The next problem was the conversion of analog video data to and from digital form. A determined effort was undertaken by the video-processing group to digitize the data directly from photographs produced from an analog signal. Although it was possible to recover everything that was on the film, there was already too great a system loss from the film recording itself. However, if the signals were recorded on magnetic tape at the time of transmission, the analog video could be digitized directly from the tape, and ground recovery losses became minimal.

After the analog tapes were converted to digital tapes, the remaining major problem was reduced to creating the computer programs which would perform the corrections, enhancements, and analyses.

The last step in the sequence was the conversion of the digital tapes to an accurate visual presentation (Ref. 1).

III. COMPUTER MANIPULATIONS

A. Corrections

The first of the computer operations is the reconstitution of the picture array from the digitized data. This process amounts to an interleaving or a sorting by computer. The picture is then packed, six digital samples of six bits each (64 gray levels), into one 36-bit word of the IBM 7094 computer. During any computer operation, the picture is brought into core memory a few video scan lines at a time from tape (or disk) and unpacked to one video brightness point per computer word. The picture is now an array in computer memory and is available for correction.

The following series of corrections evolved as a result of working with the pictures themselves. (Other photo or video systems may or may not require these operations.)

1. Geometric correction – physical straightening of photo image.

2. Photometric correction — correction of nonuniform brightness response of vidicon.

3. Random-noise removal — superposition and comparison (anticipated but not necessary for *Ranger*).

4. System-noise (periodic) removal — elimination of spurious visible frequencies superimposed on image.

5. Scan-line-noise removal — correction of nonuniform response of camera with respect to successive scan lines.

6. Sine-wave correction — compensation for attenuation of high-frequency components.

1. Geometric

The first calibration to be applied must be geometric in order to ensure the proper registration of other calibrations. This correction is determined from preflight grid measurements as well as postflight reseau measurements.

The geometric correction is measured from the distorted image of the calibration grid, which has about ten to fifteen rows per picture height and width. The corresponding video elements between these intersections are shifted by a linear interpolation to the corresponding original position. If it appears by visual inspection that the change between grid points warrants more than a single interpolation because of severe nonlinearity, then more correction points may be chosen between rows. While these shifts could be determined prior to flight, in practice, the measurements are made after success is assured. In fact, calibration and reseau-shift information are combined into one geometric correction (Fig. 1). This program is also used to reproject the picture to the normal direction (Fig. 2).

2. Photometric

If the camera characteristics as measured on the ground could withstand launch and the interplanetary voyage, their measurements could be applied to the data later. However, such an assumption cannot realistically be made. The only trustworthy method of calibration is that performed against a standard immediately before, during, and after the experimental measurements have been made. For *Ranger*, the "after" was too late; and there was no inflight calibration incorporated into the mission design for "during." (Inflight calibration was also not performed for *Mariner*.) Therefore, the preflight measurements alone had to be depended upon.

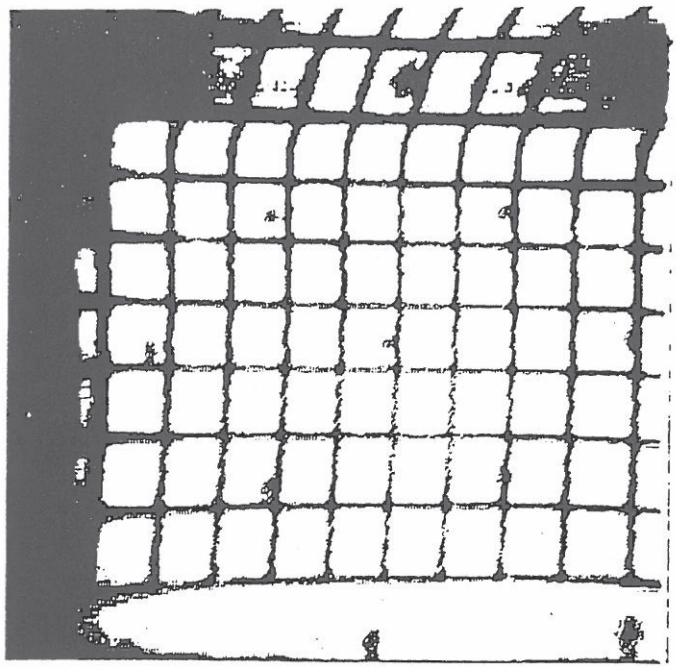

Fig. 1a. Image of a uniform grid as seen by an early *Ranger* camera

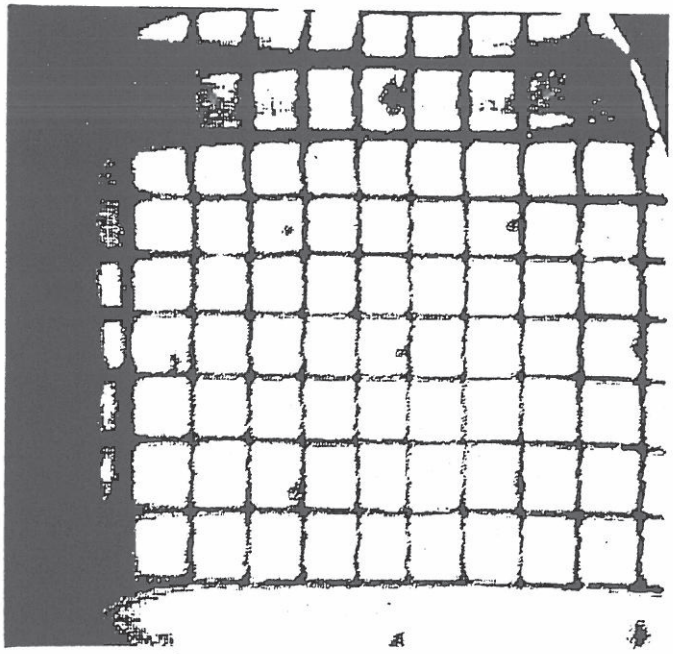

Fig. 1b. Corrected grid after moving intersections back to a square array (Note that some distortion remains in the third row as a result of extreme nonlinear distortion. Reference points could have been selected in a finer mesh to create better results.)

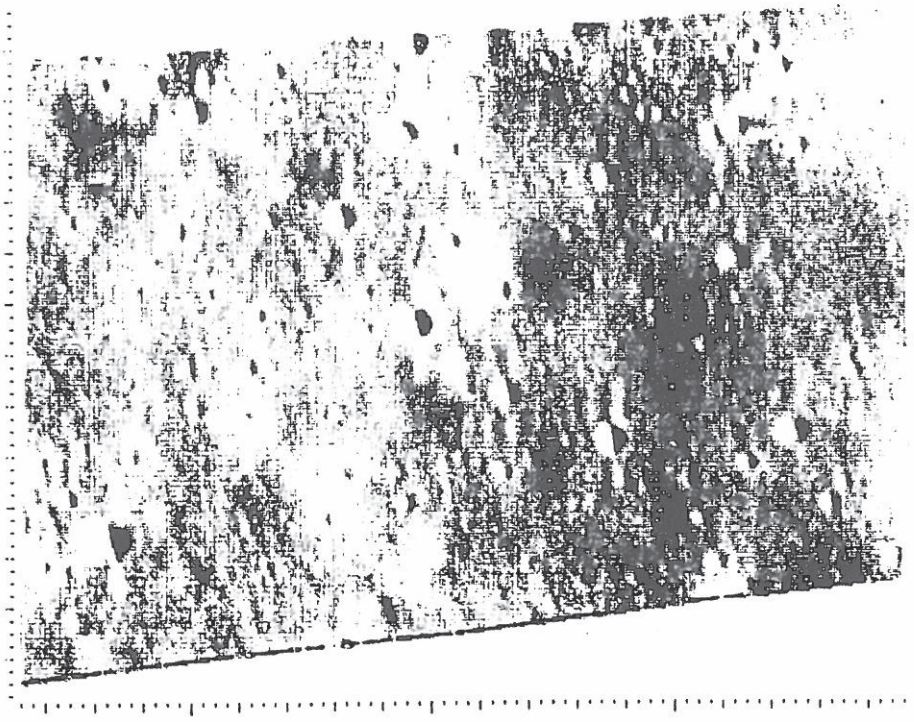

Fig. 2a. *Ranger VIII* frame reprojected using geometric-correction program as it would appear from vertical viewing

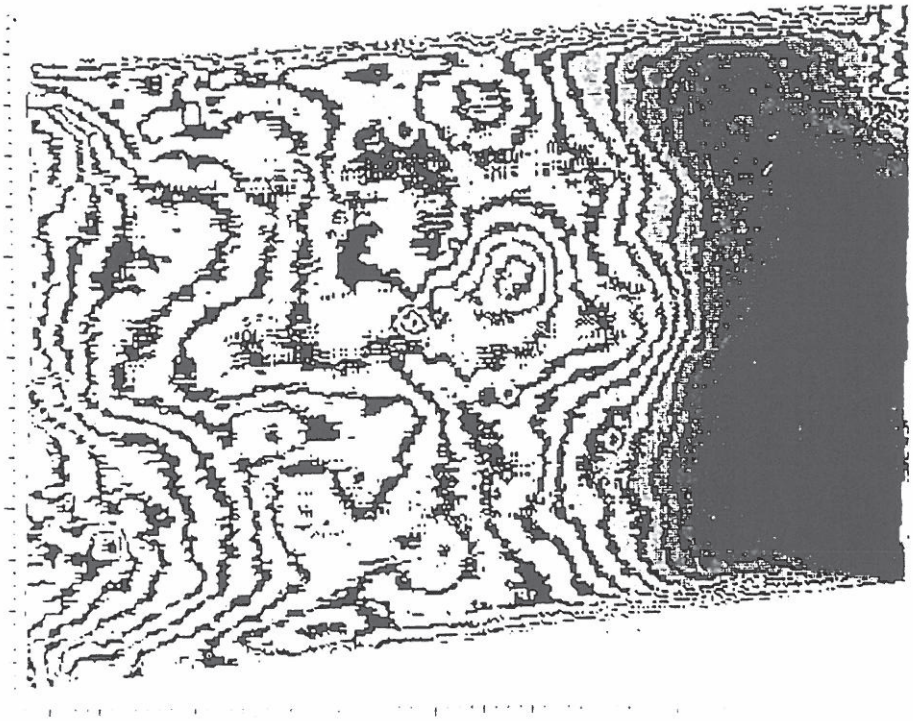

Fig. 2b. *Ranger VIII* frame converted to elevations showing contours as well as darker-appearing elevated regions

Examination of the photometric response to a uniformly lit field along a single scan line for each of several illuminations (Fig. 3) shows that the response is not uniform in either sensitivity or magnitude. Photometric measurements are made for each line over the entire picture frame. The calibration data are unique for each point of the vidicon-camera surface and must be applied individually. Since there were so many points in the *Ranger* cameras, a simple linear interpolation was used to adjust the actual data lying between calibration brightnesses. The nonuniformity in the *Ranger VII*, *VIII* and *IX* partial-scan (P) cameras, with 300 lines/frame, was not too severe. It was very pronounced in the full-scan-camera (F) frames of 1100 scan lines/frame, and in the *Mariner* data (Fig. 4). In such severe cases, very careful adjustment of the calibration data for postlaunch change in parameters is required to flatten the resultant image field. The assumption that the viewed terrain is essentially flat in brightness over the whole frame is used as the "inflight calibration." In general, the correction is performed by summing a number of frames and taking the result as an approximate gray calibration.

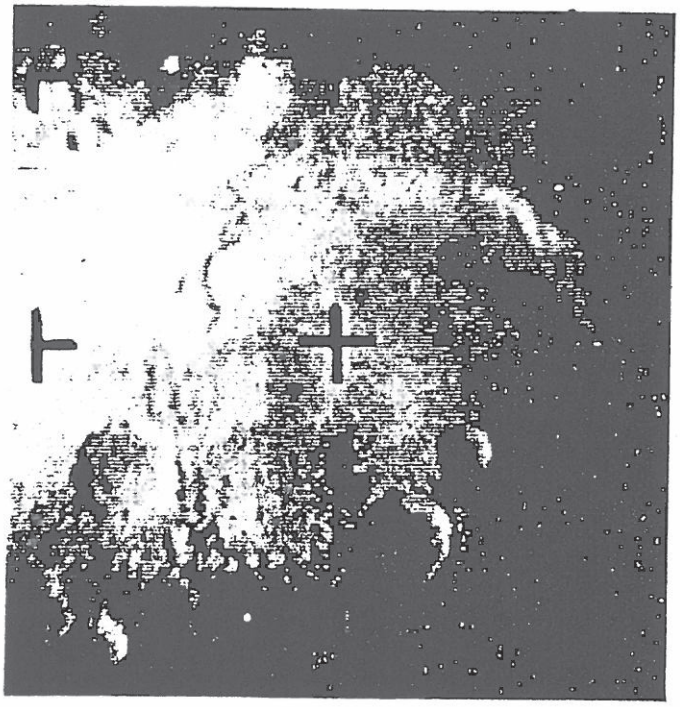

Fig. 4a. *Mariner* frame 11

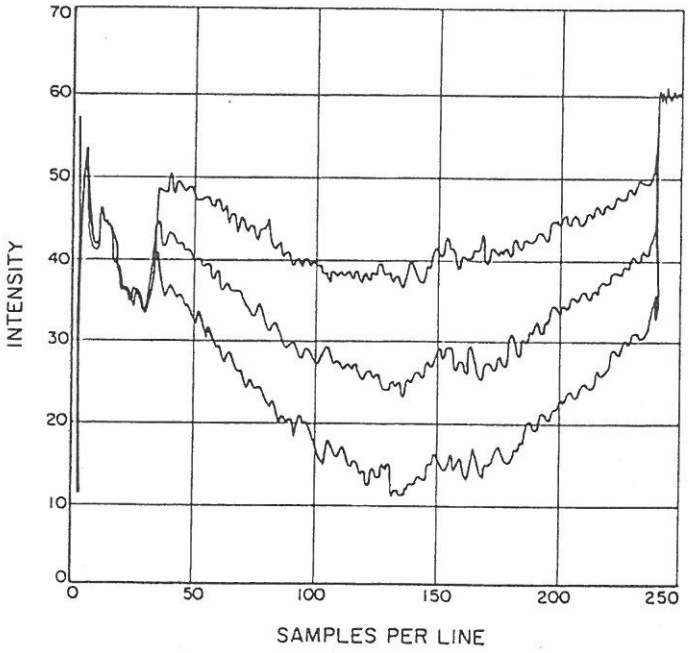

Fig. 3. Photometric calibration (Abscissa represents distance along one particular scan line — in about the middle of a video frame. Ordinate shows voltage response to three levels of light from a uniformly lit screen; white is down.)

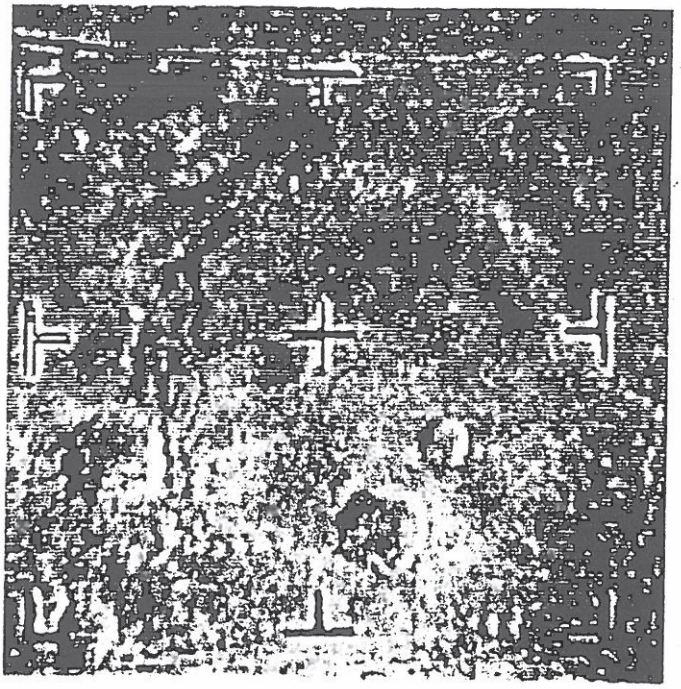

Fig. 4b. *Mariner* frame 11 after preliminary, experimental field-flattening correction and contrast enhancement

3. Random Noise

Most of the noise discovered in the *Ranger* pictures had not been anticipated. The programs for its removal were written after the data were received.

There were, however, two classes of noise which had been anticipated and for which programs were written in advance. This noise was caused by a poor signal-to-noise ratio, which created random points of bad data. In one case, the random noise gave rise to the appearance of "snow." However, this extreme change in the data can be detected, and the affected points can be replaced by the average of the neighboring points. If the amount of snow is extreme, the theoretical picture resolution is degraded by this method of clean-up; but without it, the picture would be too hard to interpret.

The second class of noise is less apparent. However, it can be detected by superimposing pictures with overlapping areas of view. This process requires a very accurate registration of data, which, in turn, involves adjustments in translation, rotation, and magnification. The magnitude of these matching parameters can be determined visually, but a computer program has been developed which registers at least two small corresponding sectors in two pictures and determines their translation differential. For local regions, a translation correlation calculation is reasonably accurate and independent of small amounts of rotation and magnification. The vector differences between the two regions are sufficient to enable the computer to calculate the three parameters of translation, rotation, and magnification for matching the whole frame.

Once the pictures are matched, one way to improve the image is by simple averaging of the repeated areas. A more powerful approach utilizes the trustworthiness of each contribution. This reliability factor is derived from the history of that point — either from its magnification or calibration adjustment, or from the validity of the measurement in terms of the noise recognized in the individual frame. This judgment associates a weight with each point, which is then incorporated into the averaging.

In addition, after the average has been computed, a comparison of the original points can be made against the neighboring points and the average. If the deviation of an original point from the average is too high, then that point can be omitted and the remaining points reaveraged. This method of majority logic is far superior to that of $\sqrt{N}$ improvement in the signal-to-noise ratio derived by straight averaging (where N is the number of averaged frames).

4. System Noise

The film records of the first *Ranger* mission were such an overwhelming success that no further improvement appeared to be possible. The indication that improvement of the results was possible was the suspicion that some loss of resolution must have taken place in the ground film recorder because of its finite recording-beam spot size. A concentrated effort was made to take the data directly from the magnetic tape, with the result that the picture obtained did indeed retrieve the resolution lost by the prime film record.

Examination of this new picture disclosed a systematic frequency superimposed upon the original image (Fig. 5). Closer inspection indicated that this noise, even though superficially of a single frequency, did in fact drift in phase throughout the picture to such an extent that no single application of the formula

$$N(x, y) = N_0 \cos 2\pi (hx + ky + \Delta)$$

(where N is the magnitude of noise at coordinates x and y in the picture, Δ represents the phase shift, and h and k are the horizontal and vertical frequency components) would match the noise at all times.

The parameters N_0, h, k, and Δ were therefore not unique. The vertical and horizontal frequency components could be selected reasonably well in a local region; amplitude N_0 and phase Δ remained to be chosen. At any particular point, the noise could be considered as a sum of cosine and sine components of the original noise, each with zero phase shift relative to that point; i.e., it was necessary to determine only the cosine component of the noise. (Note that a sine component of zero phase at the origin is zero.) This determination can be made by performing a cross-correlation of the picture against the function $N \cos 2\pi (hx + ky)$, where N is a normalizing factor and h and k are chosen approximately by visual examination of the picture. The calculation becomes

$$\rho(x_0, y_0) = N \sum_{x=-r}^{r} \sum_{y=-s}^{s} B_0 (x+x_0, y+y_0) \cos 2\pi (hx+ky) \tag{1}$$

$$\frac{1}{N} = \sum_{x=-r}^{r} \sum_{y=-s}^{s} \cos^2 2\pi (hx+ky)$$

where $B_0(x_0, y_0)$ is the original image brightness and $\rho(x_0, y_0)$ then gives the magnitude of noise contributing to that point. It should be noted that r and s are chosen somewhat arbitrarily to accommodate the computer time taken in these calculations. It should also be mentioned that the function is stored in memory as a table and not recalculated for each point.

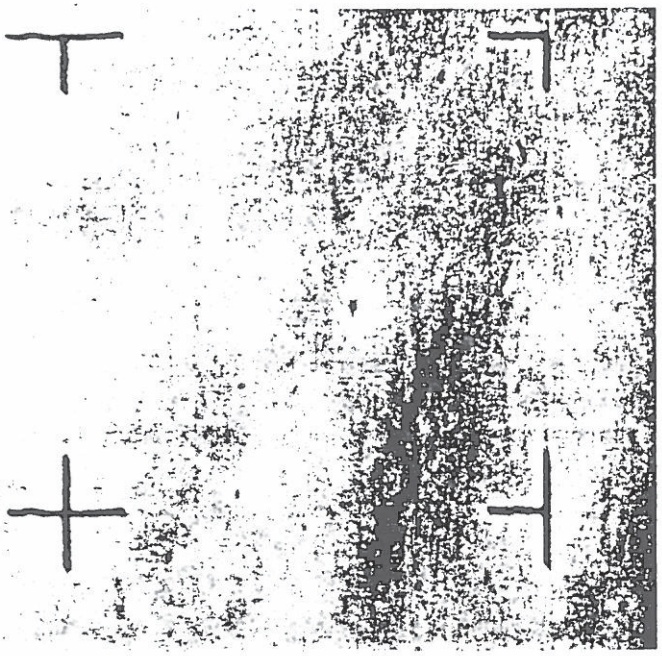

Fig. 5a. Blown-up portion of film recording from *Ranger VII* (Notice film grain and loss of resolution.)

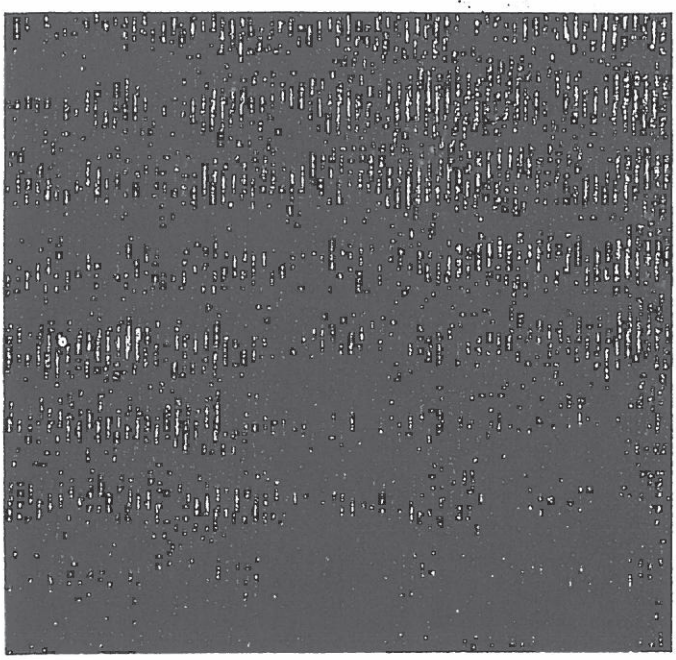

Fig. 5c. Magnitude of noise found in (b)

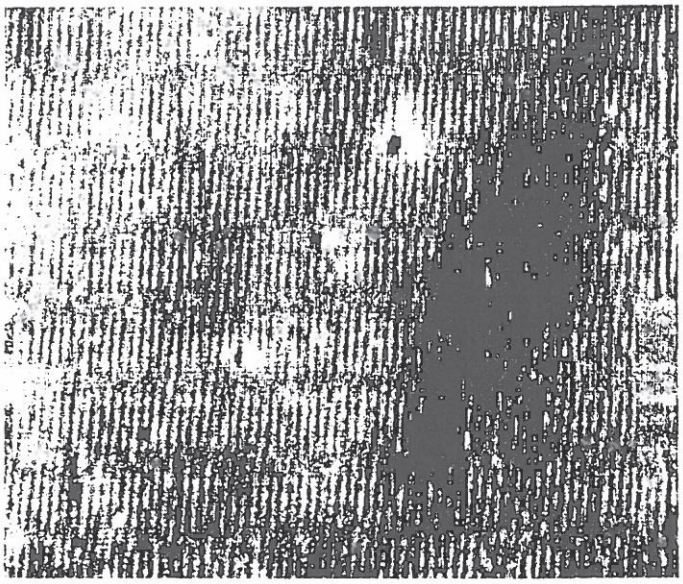

Fig. 5b. Same area from digitized data but unprocessed with respect to noise removal (Reseau mark has been removed; noise from television-camera erase cycle is visible.)

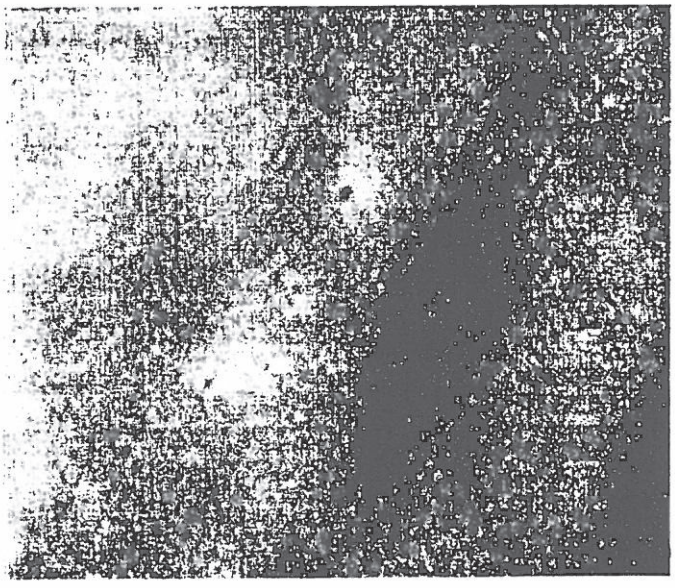

Fig. 5d. Result of subtracting noise from (b)

The correction to the picture is simply

$$B(x, y) = B_0(x, y) - \rho(x, y) \tag{2}$$

It becomes very useful to generalize these calculations in terms of the Fourier or frequency transform. For simplicity, the discussion can temporarily be kept to one dimension without immediate loss of generality. The Fourier transform of a real function in x (either time or distance), $P(x) \rightarrow A(h)$ to a frequency domain h, is

$$A(h) = \int_{-1/2}^{1/2} P(x) \cos 2\pi(hx + \Delta)dx \tag{3}$$

where $A(h)$ is the amplitude of each component of the original picture with frequency h. Where x is discrete, the integral becomes a summation. The original picture can then be represented in the frequency domain as a set of vectors whose direction normal to the base line indicates the phase angle Δ, and where A is the length of the vector for each h. This vector can point in any direction between the real and imaginary planes.

Let us consider the probable envelope of the A-vectors in the real plane only as being random but distributed (roughly uniformly) over all possible frequencies. Systematic noise, however, as found in these pictures, is clustered very heavily around a single frequency. A filter peaked near this frequency is all that is needed to clean out the noise, but if the noise is not exactly at a single frequency, then too sharp or accurate a filter will not remove all of it. Yet, too broad a filter removes too much of the picture. Subjective judgment and consideration of computer time now become factors as various trials are made to determine the optimum filter.

The easiest digital filter to design would be a very sharp one, consisting of essentially a delta function in frequency and an infinite cosine wave of a single frequency in the real domain.

The filter next in complexity as well as effectiveness would be

$$\frac{\sin 2\pi\left[(h-h_0)n\right]}{2\pi(h-h_0)n} \tag{4}$$

which in the real domain consists of a square truncation of a cosine wave of frequency h_0.

The chosen filter is of the form

$$\frac{\sin^2 2\pi\left[(h-h_0)n\right]}{4\pi^2(h-h_0)^2n^2} \tag{5}$$

which is a triangular truncation of a single frequency h_0, and the truncation factor n is related to the sharpness of cutoff.

When this filter is subtracted from the original data, a notch results at the dominant noise frequency, as seen in Fig. 6. Mathematically, the filtered frequency is positive and negative, as shown in Fig. 7, which gives rise to a cosine transform of zero phase (no sine component). Rather than multiplying the Fourier transform of the picture by this notch filter in the frequency domain and then inverse-transforming back to the real dimension, it is more practical to perform a convolution operation of the inverse transform of the filter and the picture. The convolution operation is identical to Eq. (1) for the sharp truncation and becomes Eq. (6) for the triangular truncation.

$$\rho_{TR}(x_0, y_0) = N \sum_{x=-r}^{r} \sum_{y=-s}^{s} B_0(x+x_0, y+y_0) \cos 2\pi(hx+ky) \times \left[\frac{r-|x|}{r}\right]\left[\frac{s-|y|}{s}\right]$$

$$\frac{1}{N} = \sum_{x=-r}^{r} \sum_{y=-s}^{s} \cos^2 2\pi(hx+ky) \left(\frac{r-|x|}{r}\right)\left(\frac{s-|y|}{s}\right) \tag{6}$$

5. Scan-Line Noise

The treatment of other kinds of noise requires bringing the discussion back to two dimensions in both the real and frequency domains. Among other things, television pictures are different from film in that they are scanned in some particular direction. Because not every scan line is

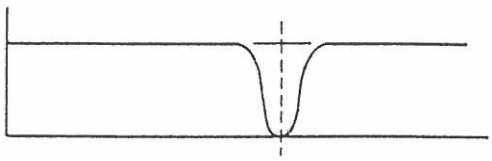

Fig. 6. Simple notch filter

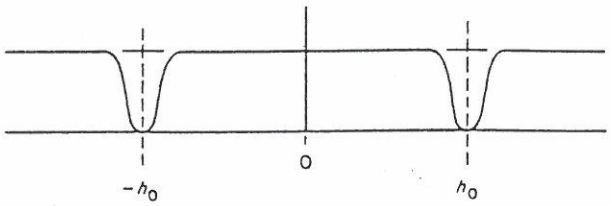

Fig. 7. Mathematically correct version of simple notch filter

carefully reproduced, noise is generated as a series of frequencies at right angles to the scan. In the two-dimensional frequency domain, these noises appear as high frequencies on the vertical axis (Fig. 8).

After some mathematical manipulation, the filter which will remove these frequencies can be described as follows. Take the average value of the scene brightness in the region of the point to be corrected. Compare the average of the scan line containing this point, and apply the difference between the scene average and the line average as a correction to the point. Application of the truncation logic of Section 4 to this filter results in a gentler response to areas more remote from the point (Fig. 9).

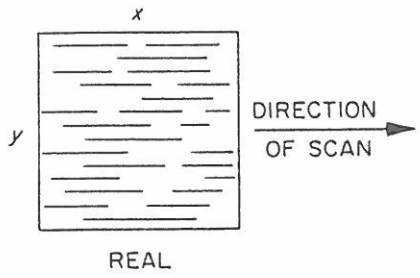

Fig. 8a. Noisy picture

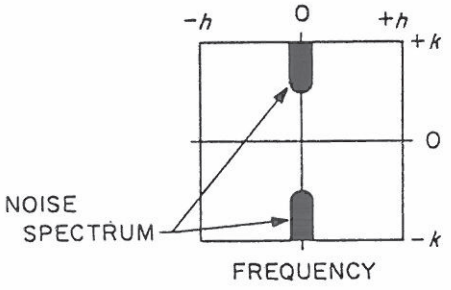

Fig. 8b. Two-dimensional frequency transform of picture

Some difficulties have arisen from features which are very sharp in contrast. These features make a significant contribution to the frequencies being removed by the filter. When the filter comes into such an area, it resonates and gives rise to false echoes of the feature. A second-order logic has been developed to be applied with this filter. The filter is turned off in the sensitive vicinity by comparing the difference between the origin and the surrounding region against some chosen threshold. When a point in the surrounding area is greater in difference than the threshold, it is replaced by the origin point. This logic is more subtle than that of standard electronic filtering because of the interaction with the real domain.

The scan-line filter is particularly useful for almost all classes of video data, but it does take about 5 min of IBM 7094 time to correct a picture of 300 × 300 elements. Proposed improvements of this computer algorithm should allow a general reduction of computer running time by at least a factor of 20. The modification amounts to sliding the filter along the scan line by adding the leading line and subtracting the trailing line from the previous calculation.

6. Sine Wave

The camera scan beam is finite in size and somewhat Gaussian in shape. If it scans a scene which has a reso-

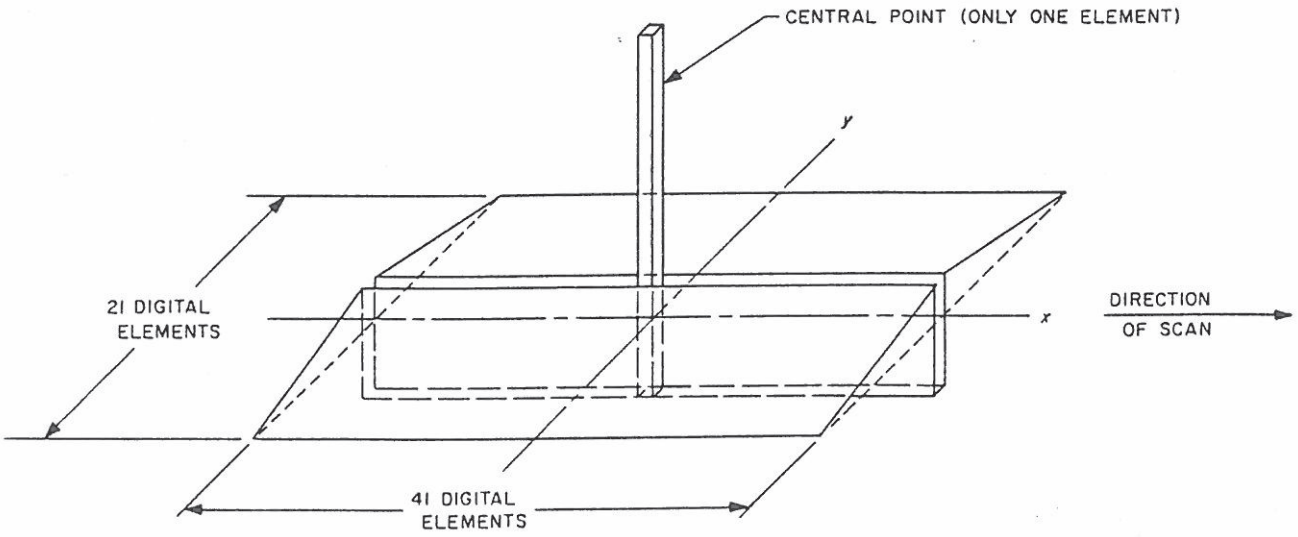

Fig. 9. Scan-line filter

lution finer than the beam spot, there will be a significant loss in the transmitted resolution; the higher frequencies will be severely attenuated, if not lost completely. In the frequency domain (using one-dimensional logic to begin with), the desired system response (modulation transfer function) would be unity for all frequencies out to the upper-limit cutoff (Fig. 10). Calibration measurements of the actual frequencies show the response illustrated in Fig. 10b. If, for each frequency h the reciprocal of the response is plotted, then the curve plotted in Fig. 10c results.

To avoid overemphasis of high-frequency noises, the upper bound of the curve is arbitrarily chosen not to exceed 5. The product of the actual- and inverse-response curves (Fig. 10d) gives a flat response out to the point where the original response has fallen to ⅕ its original value. The filtering program can again be applied, using the Fourier inverse of the reciprocal response. The convolution of this inverse function and the brightness of the original photograph enhances the higher frequencies to a point equivalent to the original scene (Fig. 11). Not only

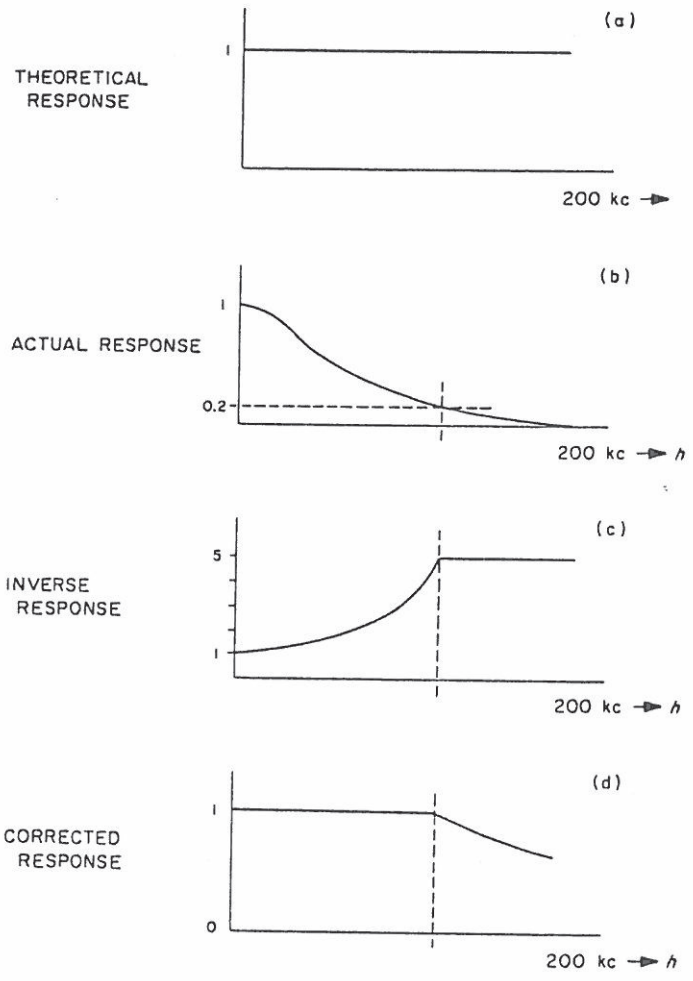

Fig. 10. System frequency-response curve

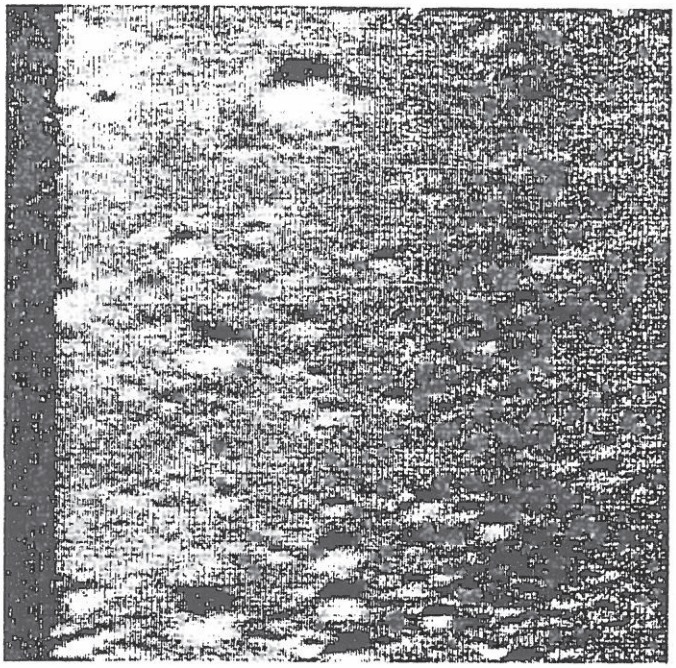

Fig. 11a. *Ranger VIII* frame after normal clean-up

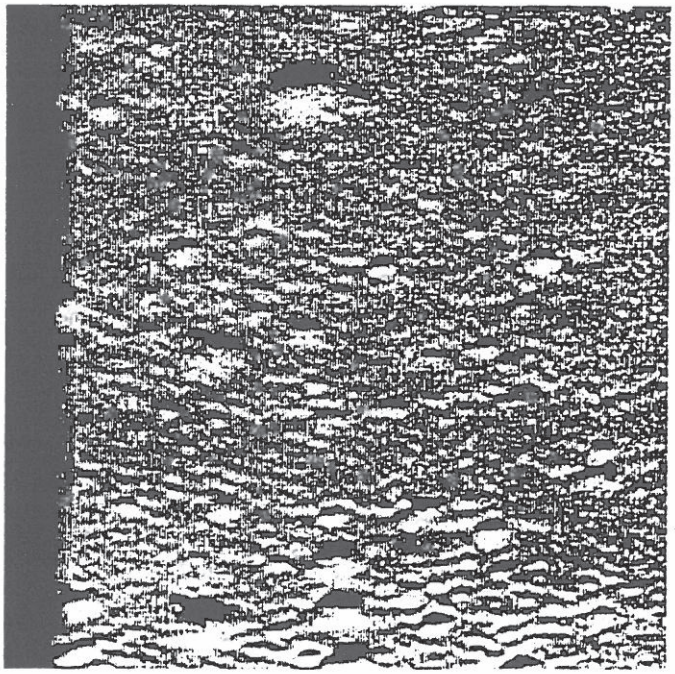

Fig. 11b. *Ranger VIII* frame with sine-wave frequency correction

is the horizontal response measured but the vertical response provides information regarding the ellipticity of the beam, and the results are incorporated into a two-dimensional filter. Typically, the correction function for the *Ranger VIII* P_3 camera appears in the real domain along each axis, as shown in Fig. 12.

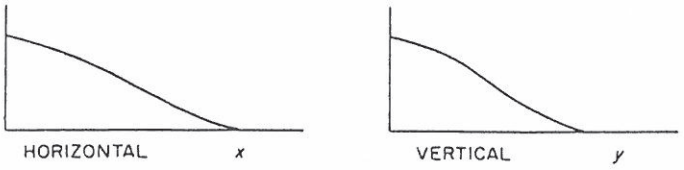

Fig. 12. Correction frequency-response curve

B. Analyses

1. Brightness-to-Slope

Once the pictures have been converted to an absolute brightness with geometric and resolution distortions removed, analysis of their contents can proceed. The concept of converting lunar brightness to slope was recently proposed by Eugene Shoemaker of the United States Geological Survey (USGS), and was worked out in detail independently by Thomas Rindfleisch of JPL (Ref. 2) and Kenneth Watson at USGS. Although this method of determining elevation has some severe theoretical limitations, it surpasses lunar stereo photography in high-resolution texture evaluation (Fig. 2).

2. Statistical

One of the operations to be performed with respect to the elevation array of the lunar landscape is that of simulated spacecraft landings. The *Surveyor* spacecraft is presently designed to accept a maximum 15-deg slope of terrain and allows for no protuberances which would nullify the effectiveness of the crushable aluminum honeycomb blocks located near the tripod landing feet. A statistical analysis of the lunar terrain has been performed which calculates the probability of distribution of slopes and protuberances relevant to the *Surveyor* spacecraft configuration.

IV. CALIBRATION

The application of computer correction methods requires knowledge of the video system. Therefore, a careful and extensive program of calibration measurements to determine the photometric, geometric, and frequency responses of each camera had to be undertaken. These measurements were recorded on magnetic tape at JPL and repeated at the launch site.

Geometric fidelity was measured by taking pictures of a two-dimensional grid. As a second-order precaution, reticle marks were placed on the camera face to establish the calibration. If the system changed after launch, the inflight measurement of reticle shift was used to recorrect the picture geometry.

Pictures of uniform white fields of known brightness levels were also taken and recorded on magnetic tape. These records provided a brightness calibration for each point on the vidicon-camera surface. In addition, each color filter (for missions such as *Mariner*) was recorded separately.

To determine the resolution of the vidicon, sine-wave charts were recorded in both the vertical and horizontal directions. A large black bar on a white field, followed by sine waves of varying frequencies, was used as the resolution target.

The shutter mechanism also had to be taken into account in the calibration of brightness. The shutter timing on alternate frames differed significantly because of the difference in speed between the forward and backward motion during a picture exposure.

V. RANGER AND MARINER RESULTS

1. Photographs from digitized tapes (not yet computer-modified) reveal higher resolution than the prime analog film records, but also some system noises (see Fig. 5).
2. Several classes of noise were removed from various frames (see Fig. 13).
3. The effect of photometric calibration was shown in field flattening; a numerically meaningful set of brightness values resulted from this correction.
4. Sine-wave correction enhanced high frequencies to give a significant increase in usable resolution (see Fig. 11).
5. A geometric-correction program was used to reorient (reproject) frames to lunar normal (see Fig. 2a).
6. Data were converted to elevations and contoured (see Fig. 2b).

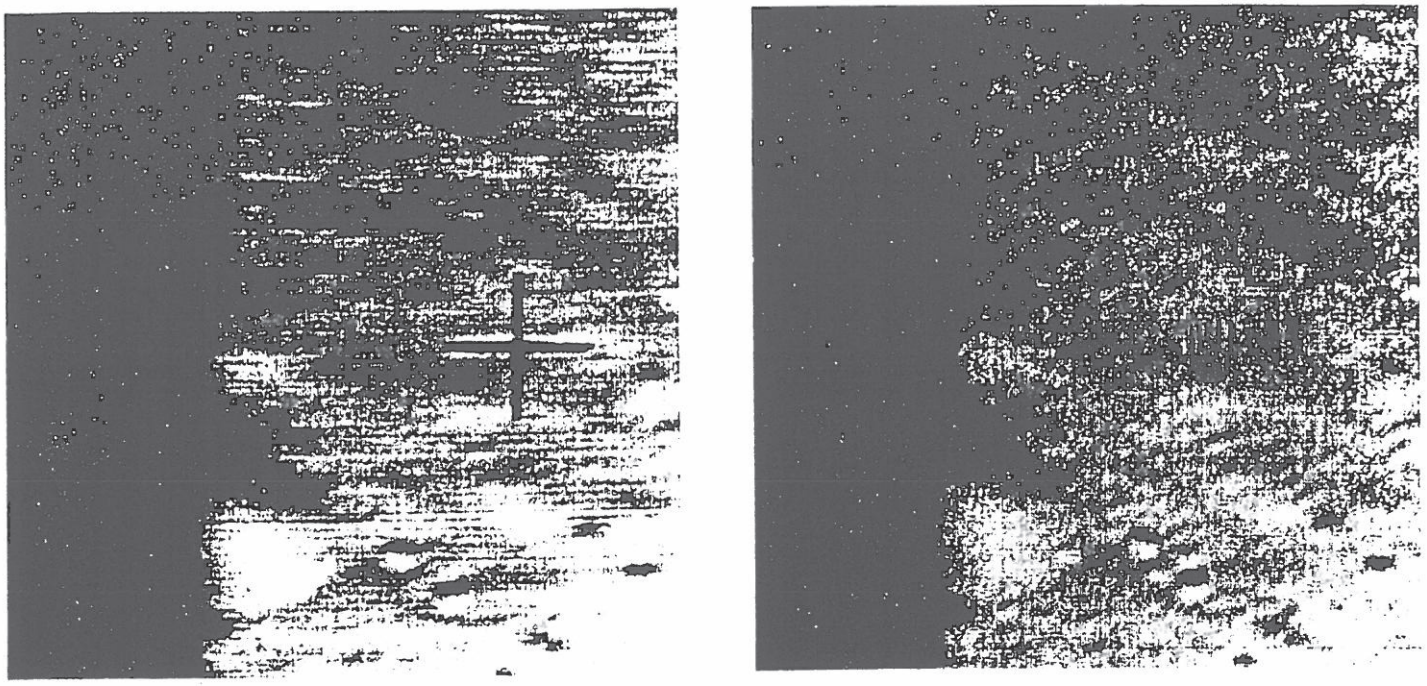

Fig. 13a. *Ranger VII* P_1 frame before (left) and after clean-up

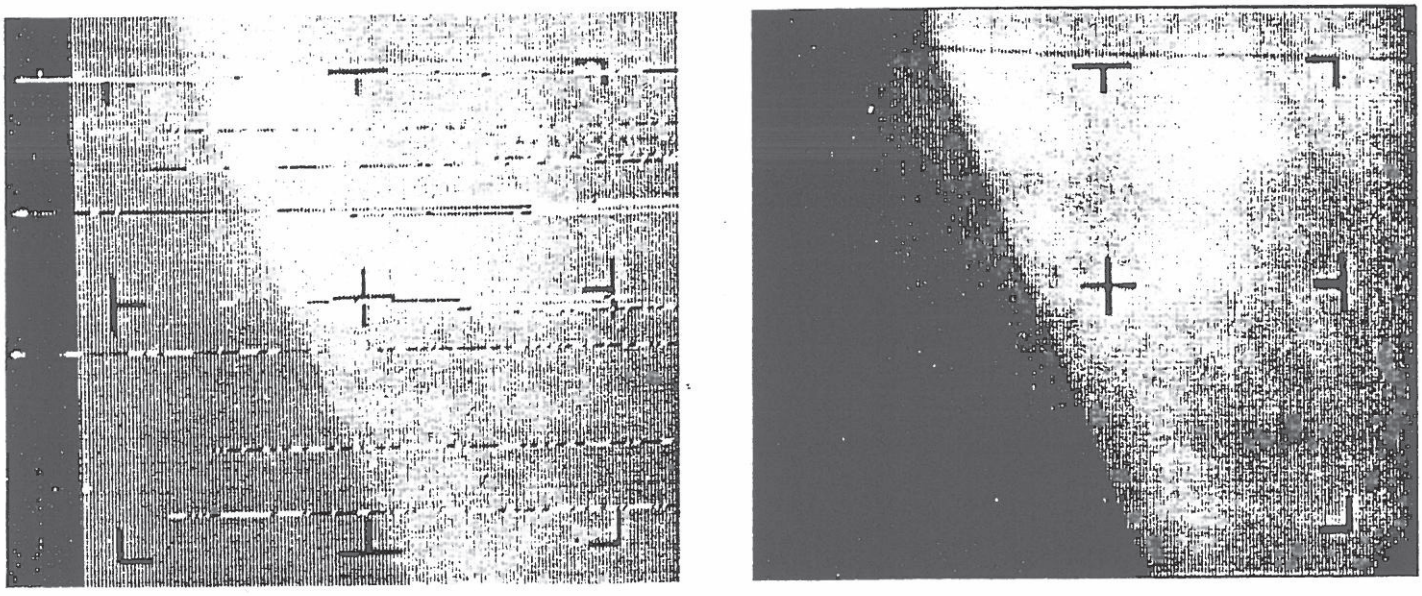

Fig. 13b. *Mariner* frame 1 before (left) and after clean-up

REFERENCES

1. Billingsley, F. C., "Digital Video Processing at JPL," Paper No. 15, *Seminar Proceedings of Electronic Imaging Techniques for Engineering, Laboratory, Astronomical and Other Scientific Measurements*, Society of Photo-Optical Instrumentation Engineers, April 26–27, 1965.

2. Rindfleisch, T. C., *A Photometric Method for Deriving Lunar Topographic Information*, Technical Report No. 32-786, Jet Propulsion Laboratory, Pasadena, California, September 15, 1965.

APPENDIX

The following are simplified examples of (1) a two-dimensional scan-noise line filter and (2) a one-dimensional high-frequency recovery filter.

The computer presently uses a 21 × 41-element array; obviously, the 3 × 3 array (used in the line filter) does not work as well as the larger matrix but is still effective.

The high-frequency enhancement filter operates identically to the periodic-noise filter, but the example presented here has the added complexity of illustrating the determination of the frequencies to be enhanced and the extent of enhancement provided.

Example 1

Let us construct a simple scan-line filter F of a 3 × 3 array:

$$F(x,y) = n_1 \begin{vmatrix} 1 & 1 & 1 \\ 1 & 1 & 1 \\ 1 & 1 & 1 \end{vmatrix} - n_2 \begin{vmatrix} 0 & 0 & 0 \\ 1 & 1 & 1 \\ 0 & 0 & 0 \end{vmatrix} + \begin{vmatrix} 0 & 0 & 0 \\ 0 & 1 & 0 \\ 0 & 0 & 0 \end{vmatrix}$$

$$= \begin{vmatrix} \frac{1}{9} & \frac{1}{9} & \frac{1}{9} \\ \frac{1}{9} & \frac{1}{9} & \frac{1}{9} \\ \frac{1}{9} & \frac{1}{9} & \frac{1}{9} \end{vmatrix} - \begin{vmatrix} 0 & 0 & 0 \\ \frac{1}{3} & \frac{1}{3} & \frac{1}{3} \\ 0 & 0 & 0 \end{vmatrix} + \begin{vmatrix} 0 & 0 & 0 \\ 0 & 1 & 0 \\ 0 & 0 & 0 \end{vmatrix}$$

$$= \begin{vmatrix} \frac{1}{9} & \frac{1}{9} & \frac{1}{9} \\ -\frac{2}{9} & \frac{7}{9} & -\frac{2}{9} \\ \frac{1}{9} & \frac{1}{9} & \frac{1}{9} \end{vmatrix}$$

or

F (y \ x)	−1	0	1
−1	$\frac{1}{9}$	$\frac{1}{9}$	$\frac{1}{9}$
0	$-\frac{2}{9}$	$\frac{7}{9}$	$-\frac{2}{9}$
1	$\frac{1}{9}$	$\frac{1}{9}$	$\frac{1}{9}$

where $1/n_1$ = the number of elements in the filter array ($n_1 = \frac{1}{9}$), and $n_2 = n_1 \times$ the number of rows in the filter array ($n_2 = n_1 \times 3 = \frac{1}{3}$).

As a test application of filter F on a received noisy signal B, consider a 6 × 6 array of numbers representing brightness A. To A add some scan-line noise N to produce received image B.

A (y \ x)	1	2	3	4	5	6
1	3	4	6	4	3	1
2	5	7	3	2	1	2
3	6	1	6	3	2	1
4	5	3	3	4	4	3
5	3	1	8	3	1	4
6	4	2	3	6	2	3

N (y \ x)	1	2	3	4	5	6
1						
2	−1	−1	−1	−1	−1	−1
3	3	3	3	3	3	3
4						
5	−1	−1	−1	−1	−1	−1
6						

B (y \ x)	1	2	3	4	5	6
1	3	4	6	4	3	1
2	4	6	2	1	0	1
3	9	4	9	6	5	4
4	5	3	3	4	4	3
5	2	0	7	2	0	3
6	4	2	3	6	2	3

Perform a convolution of filter F and array B to give approximate recovery R back to A:

$$R(x_0, y_0) = \sum_{x=-1}^{1} \sum_{y=-1}^{1} B(x_0+x, y_0+y)\, F(x, y)$$

$$\text{for each } \begin{cases} x_0 = 2 \text{ to } 5 \\ y_0 = 2 \text{ to } 5 \end{cases}$$

R (y \ x)	2	3	4	5
2	7	4	4	2
3	1	7	3	3
4	4	4	5	4
5	0	7	2	1

The error of recovery is $E = R - A$.

E (y \ x)	2	3	4	5
2	0	1	2	1
3	0	1	0	1
4	1	1	1	0
5	−1	−1	−1	0

Effectiveness may be measured by comparing average noise $|\overline{N}|$ against error matrix $|\overline{E}|$ over the range $x = 2$ to 5 and $y = 2$ to 5.

$$|\overline{N}| = \frac{1}{16} \sum_{x=2}^{5} \sum_{y=2}^{5} |N(x,y)| = 1.25$$

$$|\overline{E}| = \frac{1}{16} \sum_{x=2}^{5} \sum_{y=2}^{5} |E(x,y)| = 0.75$$

Hence, a decided improvement is shown for a very small filter.

Example 2

Let us consider a one-dimensional scene in x with brightness $A(x)$.

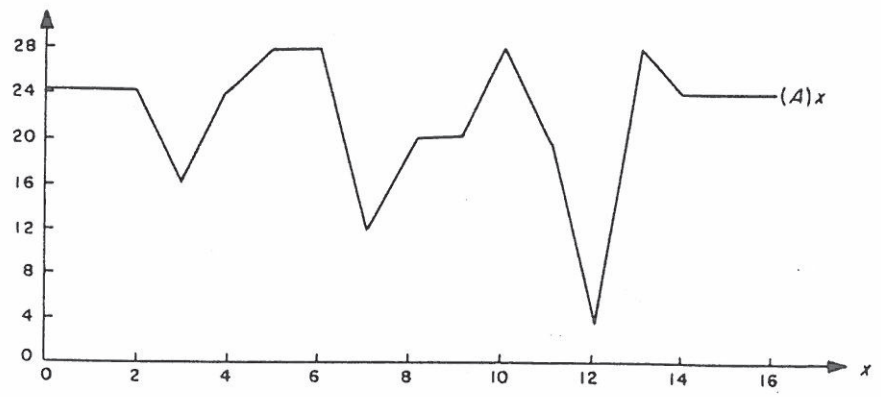

Let A be scanned by a beam with the response shape $S(x)$:

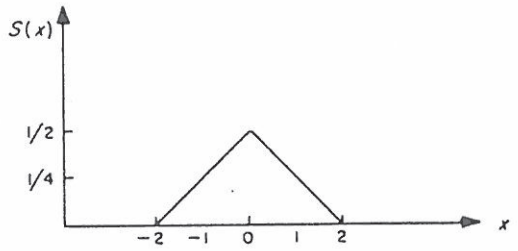

The transmitted brightness is a convolution of A and S to form $B(x)$:

$$B(x) = \sum_{x=-1}^{1} A(x_n + x)\, S(x) \qquad \text{for each } x_n = 1 \text{ to } 15$$

There is a visible drop in resolution from A to B.

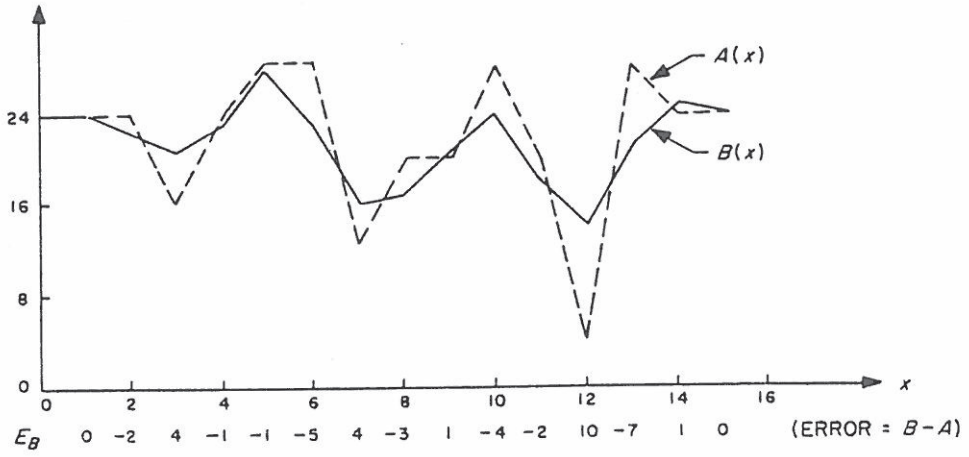

The Fourier transform of $S(x)$ is $(\sin 2\pi h)^2/(2\pi h)^2 = T_S(h)$.

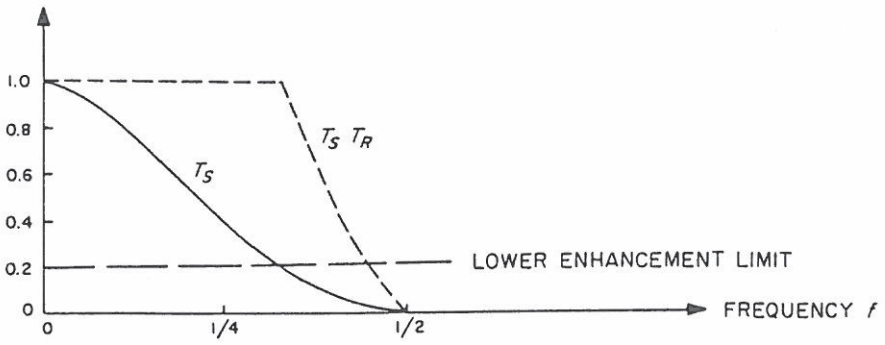

Now, let us take the reciprocal of T_S,

$$T_R(h) = \frac{1}{T_S}$$

but $T_R \leqslant 5$ is an arbitrary upper bound to avoid noise enhancement.

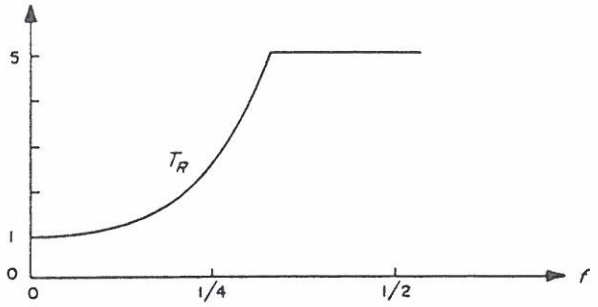

Let us subtract T_R from 5 and take an inverse Fourier transform to real space.

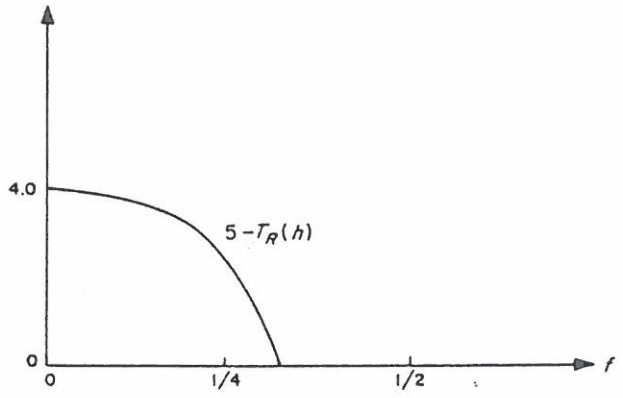

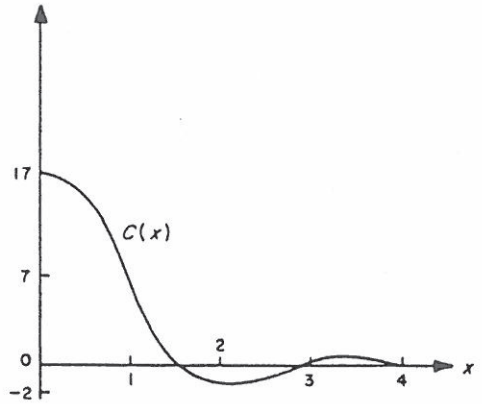

We now have an unnormalized correction function C.

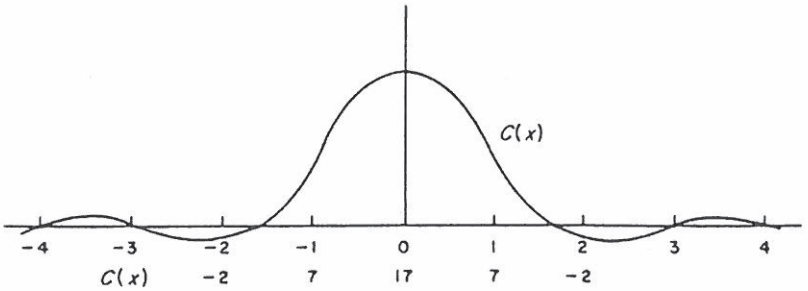

In order to convert C into a filter, an adjustment must be made for the fact that the transform of this function was subtracted from 5 in the frequency domain. Two constants, K_1 and K_2, must be determined for the filter.

$$F(x) = K_1\,\delta(0) - K_2\,C(x)$$

$$\text{where } \delta(0) \text{ is a delta function } \begin{cases} = 1 \text{ for } x = 0 \\ = 0 \text{ for } x \neq 0. \end{cases}$$

The convolution of $F(x)$ and a brightness of very high frequency will cause $C(x)$ to drop out, and an enhancement factor of 5 will result (see T_R at high frequency).

Therefore,

$$5 = F = K_1\,\delta(0)$$

$$K_1 = 5$$

The convolution of $F(x)$ and a constant brightness of magnitude 1 should give an enhancement factor of 1 [see $T_R(0)$].

$$1 = \sum_{x=-2}^{2} 1\,F(x) = \sum_{x=-2}^{2} [5\,\delta(0) - K_2\,C(x)]$$

$$= 5 - K_2\,[-2 + 7 + 17 + 7 - 2]$$

Therefore,

$$K_2 = \frac{4}{27}$$

$$F(x) = 5\,\delta(0) - \frac{4}{27}C(x)$$

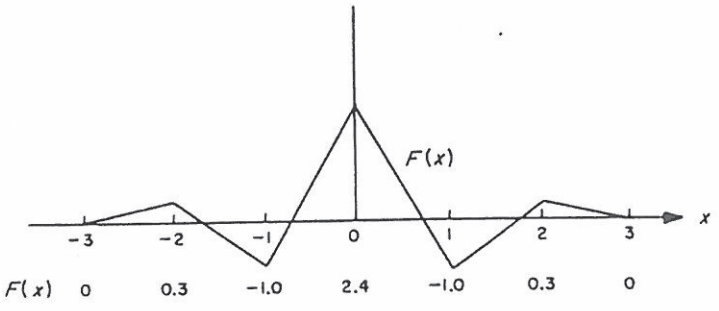

When a convolution is performed between $F(x)$ and $B(x)$, the result $R(x)$ represents a reconstruction of $A(x)$ to the degree permitted by the enhancement of the

higher frequencies, as indicated by T_S T_R.

$$R(x_0) = \sum_{x=-2}^{2} B\,(x_0 + x)\,F(x)$$

for $x_0 = 1$ to 15

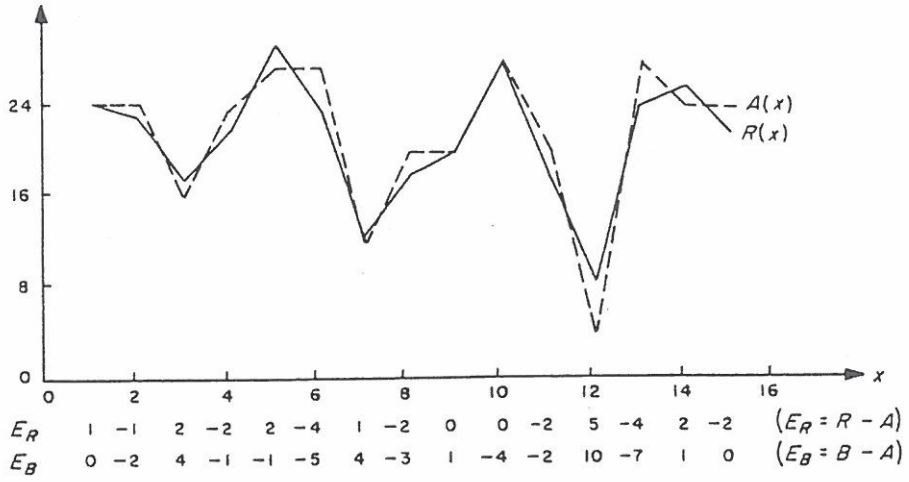

Compare the error E_B caused by the scanning beam against the error E_R remaining in the reconstructed image.

$$|\overline{E_B}| = \frac{1}{15}\sum_{x=1}^{15} |E_B| = \frac{45}{15} = 3.0$$

$$|\overline{E_R}| = \frac{1}{15}\sum_{x=1}^{15} |E_R| = \frac{30}{15} = 2.0$$

This is a distinct improvement. Visual comparison of the plots of A vs B and A vs R also shows that R matches A much better than does B.

ACKNOWLEDGMENTS

The author would like to express his appreciation for the work performed by Fred Billingsley and his group in connection with the hardware involved in the conversion of analog data to computer-compatible digital form and the conversion of processed digital tapes to high-quality pictures on film. In addition, the efforts of Frank Lyle and Howard Frieden of the Mesa Scientific Corporation in the area of computer programming are gratefully acknowledged. In a parallel operation, which incorporated both a hardware and a software analysis of *Mariner* video data, John Morecroft has also made strong contributions.